Supplementary information

Recessive mutations in *DGKE* cause atypical hemolytic-uremic syndrome

Mathieu Lemaire[1,2,24], Véronique Frémeaux-Bacchi[3,4,24], Franz Schaefer[5,6], Murim Choi[1,2,7], Wai Ho Tang[8], Moglie Le Quintrec[4], Fadi Fakhouri[9], Sophie Taque[10], François Nobili[11], Frank Martinez[12], Weizhen Ji[1,2], John D. Overton[1,7], Shrikant M. Mane[1,7], Gudrun Nürnberg[13], Janine Altmüller[13], Holger Thiele[13], Denis Morin[14], Georges Deschenes[15], Véronique Baudouin[15], Brigitte Llanas[16], Laure Collard[17], Mohammed A. Majid[18], Eva Simkova[18], Peter Nürnberg[13,19,20], Nathalie Rioux-Leclerc[21], Gilbert W. Moeckel[22], Marie Claire Gubler[23], John Hwa[8], Chantal Loirat[15] & Richard P. Lifton[1,2,7]

[1]Department of Genetics, Yale University School of Medicine, New Haven, Connecticut, USA.
[2]Howard Hughes Medical Institute, Yale University School of Medicine, New Haven, Connecticut, USA.
[3]Department of Immunology, Assistance Publique–Hôpitaux de Paris, Hôpital Européen Georges-Pompidou, Paris, France.
[4]UMRS 872, Centre de Recherche des Cordeliers, Paris, France.
[5]Division of Pediatric Nephrology and KFH Children's Kidney Center, Heidelberg University Medical Center, Heidelberg, Germany.
[6]Center for Pediatrics and Adolescent Medicine, Heidelberg University Medical Center, Heidelberg, Germany.
[7]Yale Center for Mendelian Genomics, Yale University School of Medicine, New Haven, Connecticut, USA.
[8]Department of Internal Medicine, Yale Cardiovascular Research Center, Section of Cardiovascular Medicine, Yale University School of Medicine, New Haven, Connecticut, USA.
[9]Department of Nephrology, CHU Nantes, Nantes, France.
[10]Department of Pediatrics, CHU Rennes, Rennes, France.
[11]Department of Pediatrics, CHU Besançon, Besançon, France.
[12]Department of Nephrology, Assistance Publique–Hôpitaux de Paris, Hôpital Necker-Enfants Malades, Paris, France.
[13]Cologne Center for Genomics, University of Cologne, Cologne, Germany.
[14]Department of Pediatric Nephrology, CHU Montpellier, Montpellier, France.
[15]Department of Pediatric Nephrology, Assistance Publique–Hôpitaux de Paris, Hôpital universitaire Robert-Debré, Paris, France.
[16]Department of Pediatric Nephrology, CHU Bordeaux, Bordeaux, France.
[17]Department of Pediatrics, CHC Liège, Liège, Belgique.
[18]Department of Pediatrics, Pediatric Nephrology Unit, Dubai Hospital, Dubai, UAE.
[19]Center for Molecular Medicine Cologne, University of Cologne, Cologne, Germany.
[20]ATLAS Biolabs GmbH, Berlin, Germany.
[21]Department of Pathology, CHU Rennes, Rennes, France.
[22]Renal Pathology and Electron Microscopy Laboratory, Yale University School of Medicine, New Haven, Connecticut, USA.
[23]INSERM U983, Hôpital Necker-Enfants Malades, Paris, France.
[24]VFB and ML contributed equally to the work.

Correspondence should be addressed to Véronique Frémeaux-Bacchi (veronique.fremeaux-bacchi@egp.aphp.fr) or Richard P Lifton (richard.lifton@yale.edu).

10 supplementary figures &
5 supplementary tables

TABLE OF CONTENTS FOR SUPPLEMENTARY INFORMATION

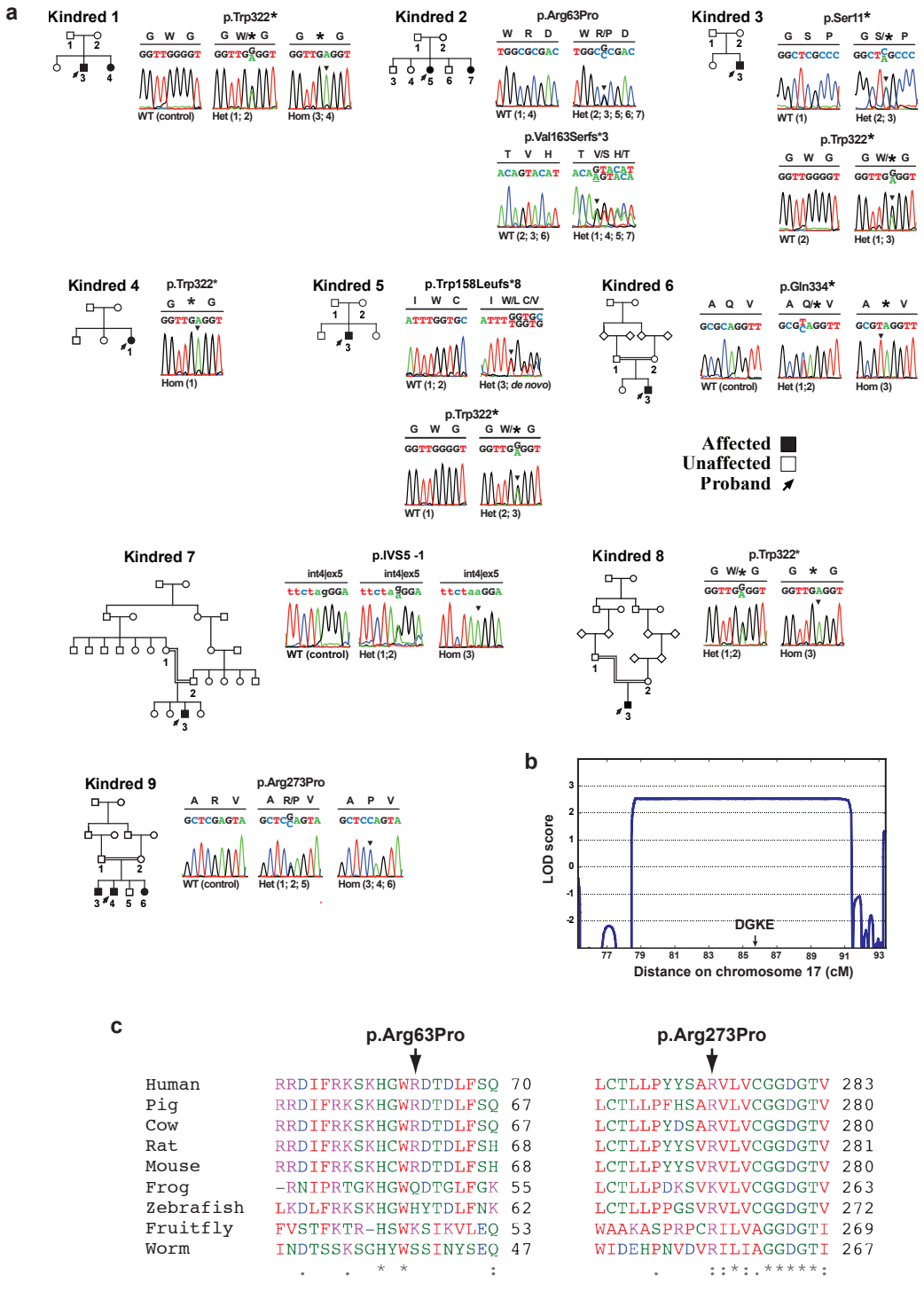

Supplementary Figure 1 *DGKE* mutations in 9 kindreds with aHUS. (**a**) Pedigree structures and Sanger sequence chromatograms from the 9 aHUS kindreds with DGKE mutations are shown. Affected subjects are denoted by filled symbols and arrows identify probands. Chromatograms show sequences indicated kindred members (subject # in parentheses) or control subjects. Above each chromatogram, the sequence of the encoded protein is shown in single letter code; intron sequences are shown in lower case font. The variants found in affected subjects are indicated by arrowheads. ex, exon; int, intron; IVS, intervening sequence; WT, wildtype. (**b**) Detailed view of the linkage peak for kindred 9. A maximum multipoint LOD score of 2.53 was observed at the chromosomal segment 17q21.31-q23.3. Genetic distances, in centiMorgan (cM), are based on deCODE map. *DGKE* position indicated by arrow. (**c**) Amino acid alignment of DGKE in multiple species in the segments including the missense mutations p.Arg63Pro and p.Arg273Pro seen in kindreds 2 and 9, respectively. Multiple alignments were performed with ClustalW2 (baseline settings). Accession codes used available in main text.

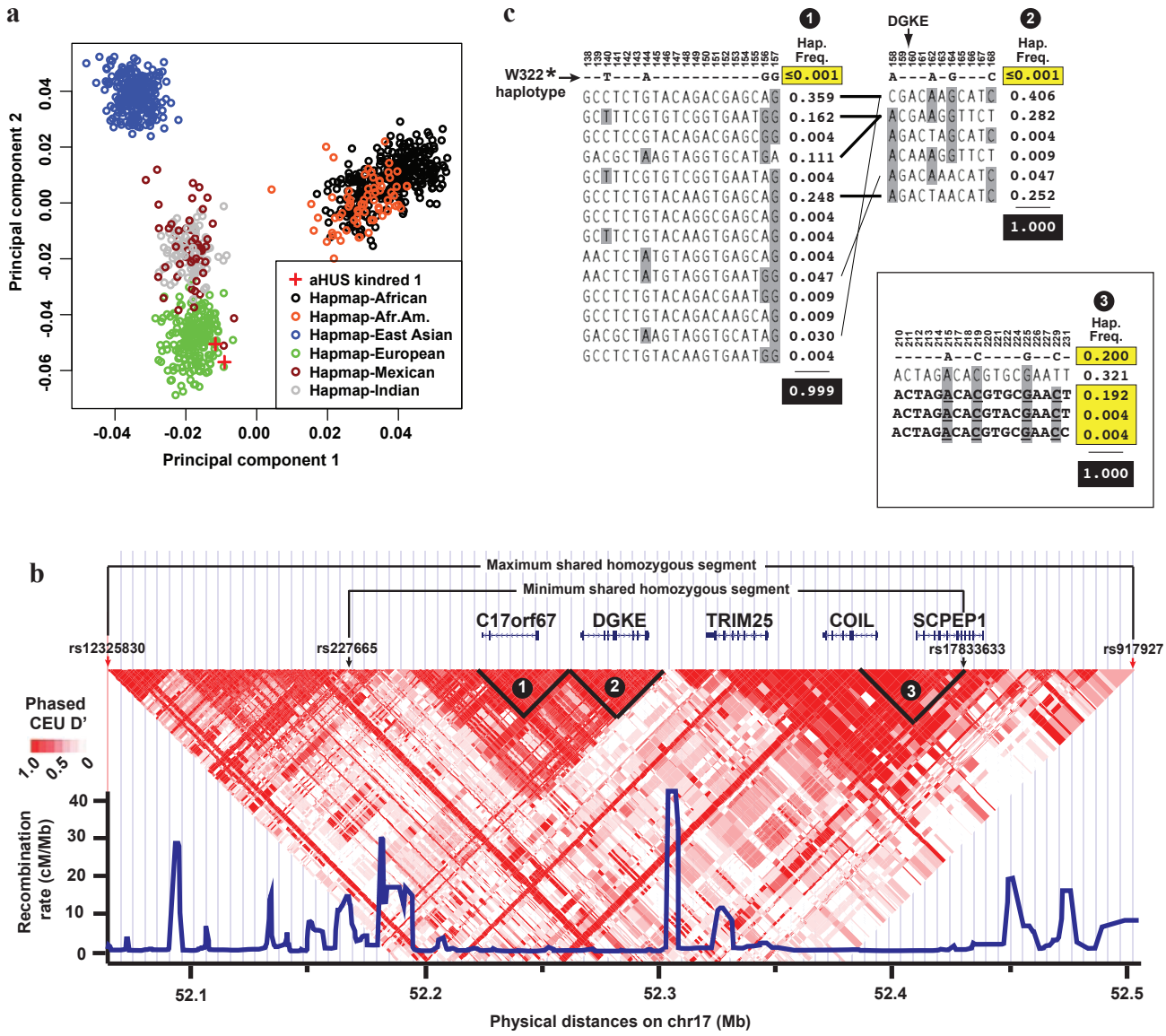

Supplementary Figure 2 Characterization of the *DGKE* p.Trp322*–associated haplotype. (**a**) Principal component analysis (PCA) of subjects from kindred 1 (1-3 and 1-4) with homozygous *DGKE* p.Trp322* mutation. Tag SNPs from exome sequences of subjects homozygous for *DGKE* p.Trp322* were combined with HapMap SNP data and PCA was performed as described in Methods. The results demonstrate that these individuals (red crosses) strongly cluster with individuals of European ancestry. (**b**) Linkage disequilibrium near *DGKE*. Hedrick's multi-allelic D' for linkage disequilibrium for SNPs in CEU from HapMap Phase II data is shown (Hg18). The physical distance (Mb) and recombination rate (cM/Mb) from HapMap Phase II genetic map are indicated. Shown above are the minimum and maximum homozygous segments shared among 3 apparently unrelated aHUS subjects homozygous for *DGKE* p.Trp322*. Genotypes for SNPs across this interval in these 3 subjects are shown in **Supplementary Table 5**. The location of 4 SNPs from this table is indicated. Haplotypes from blocks of LD labeled 1, 2, and 3 are shown in panel (**c**). D' between LD blocks 1 and 2 is 1, and between 1/2 and 3 is 0.18. (**c**) Haplotype frequencies for LD blocks 1,2 and 3. *DGKE* is in block 2 (arrow). Each row shows haplotypes in the CEU population with its frequency from HapMap CEU subjects. Four tag SNPs were genotyped in both blocks 1 and 2. Each tag SNP is identified by a number in bold located above the LD block, which corresponds to one row in **Supplementary Table 5**. The base indicated above each tag SNP indicates the allele found on the shared haplotype; these alleles are highlighted with a gray box in each haplotype on which they occur ("-" indicates tag SNPs that were not genotyped). The combined frequencies of all haplotypes containing all 4 shared alleles in each block are highlighted in yellow. The shared haplotype harboring the *DGKE* p.Trp322* mutation is not found among HapMap chromosomes. Since the sum of all possible CEU haplotypes frequencies is ~99.9% for each LD block (black box), the frequency of the patients' haplotype is at most 0.1% in the CEU cohort (yellow box). A third LD block from the shared interval (labeled "3") is shown in the box, illustrating that the shared haplotype in this segment is common in CEU.

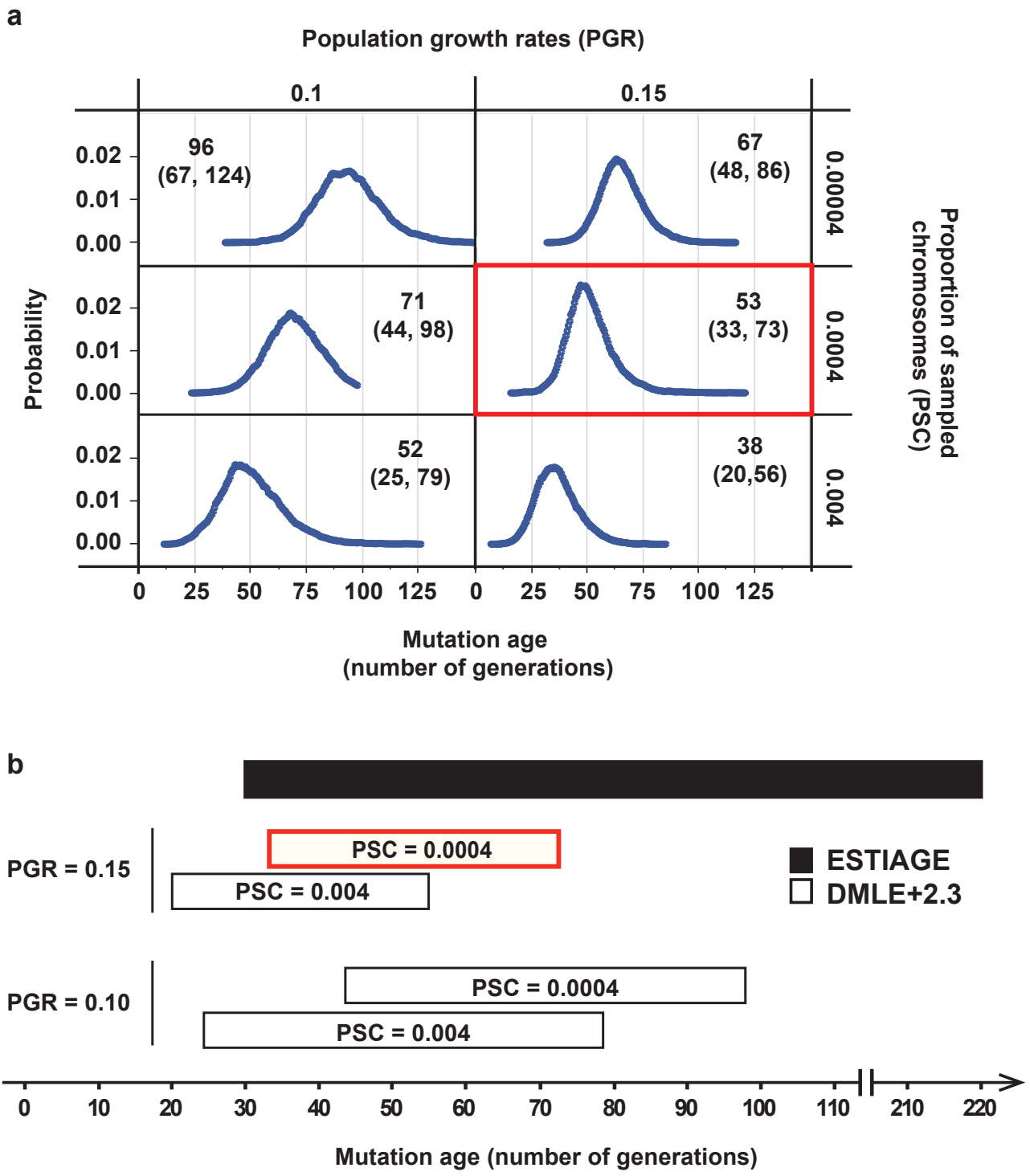

Supplementary Figure 3 Estimation of the mutation age for *DGKE* p.Trp322*. (**a**) Distribution of probable mutation ages from DMLE+2.3 is shown as population growth rate (PGR) and proportion of sampled chromosomes (PSC) are varied across most likely estimates. The result from the best estimate of these parameters is indicated by the red box. The mean mutation age is also indicated on each graph, along with the calculated 95% confidence interval (in parentheses). (**b**) This panel overlays the 95% confidence interval data from in **a** for PGRs of 0.10 and 0.15 and various PSC values with that of the 95% confidence interval for the estimated mutation age obtained with ESTIAGE software.

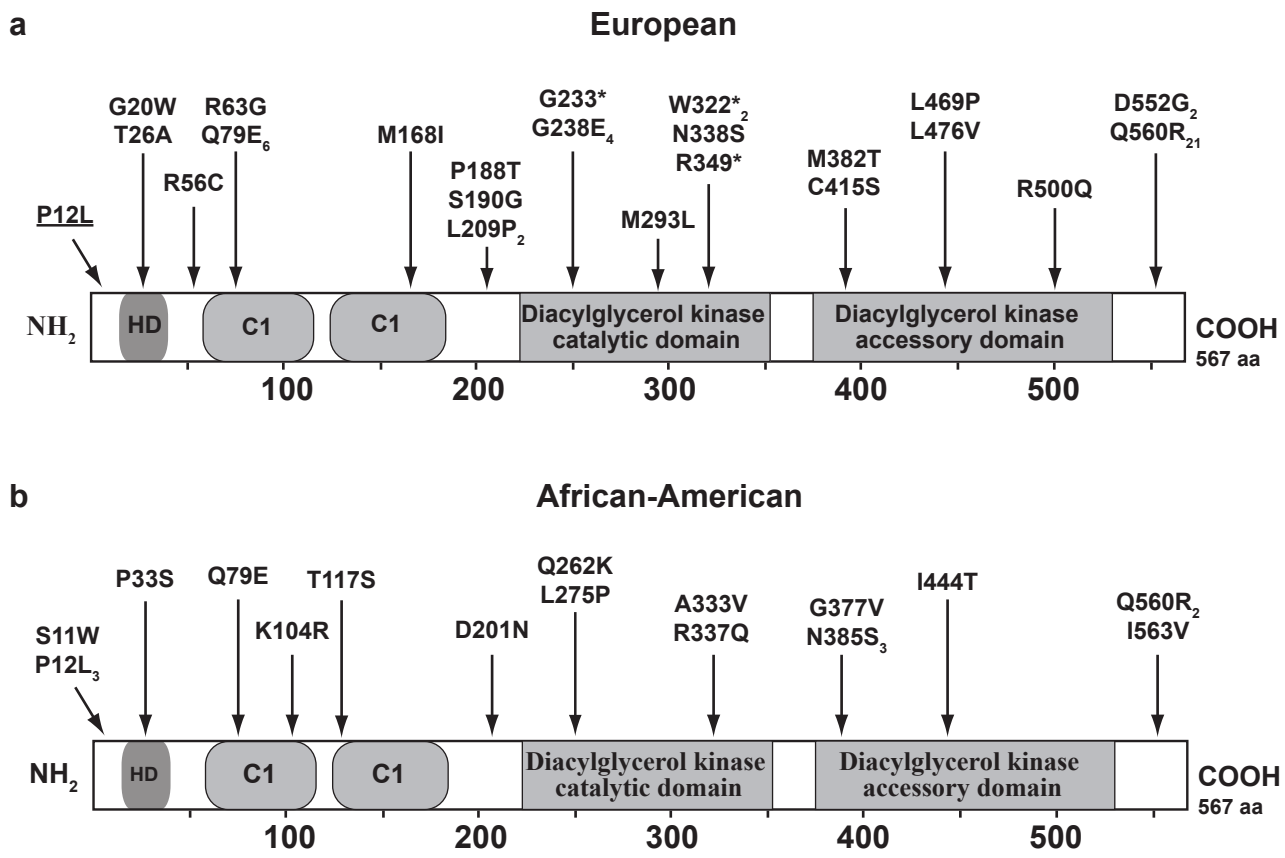

Supplementary Figure 4 Location of the heterozygous *DGKE* variants with minor allele frequencies < 1% observed in unaffected European-American. (**a-b**) Schematic representation of DGKE showing the positions of all heterozygous mutations found in 8,475 control exomes from subjects of European (**a**) or African-American (**b**) descent relative to the cDNA structure and known functional domains. There is a single subject harboring homozygous variant *DGKE* p.Pro12Leu (underlined). For variants seen more than once, the number of subjects observed is indicated by the numbers in subscript. All other variants were unique. HD, hydrophobic domain; C1, C1 domain. (**c**) Amino acid sequence alignment of the segment of DGKE including missense variant p.Pro12Leu that is homozygous in one control subject. Multiple alignments were performed with ClustalW2 (baseline settings). Accession codes used available in main text.

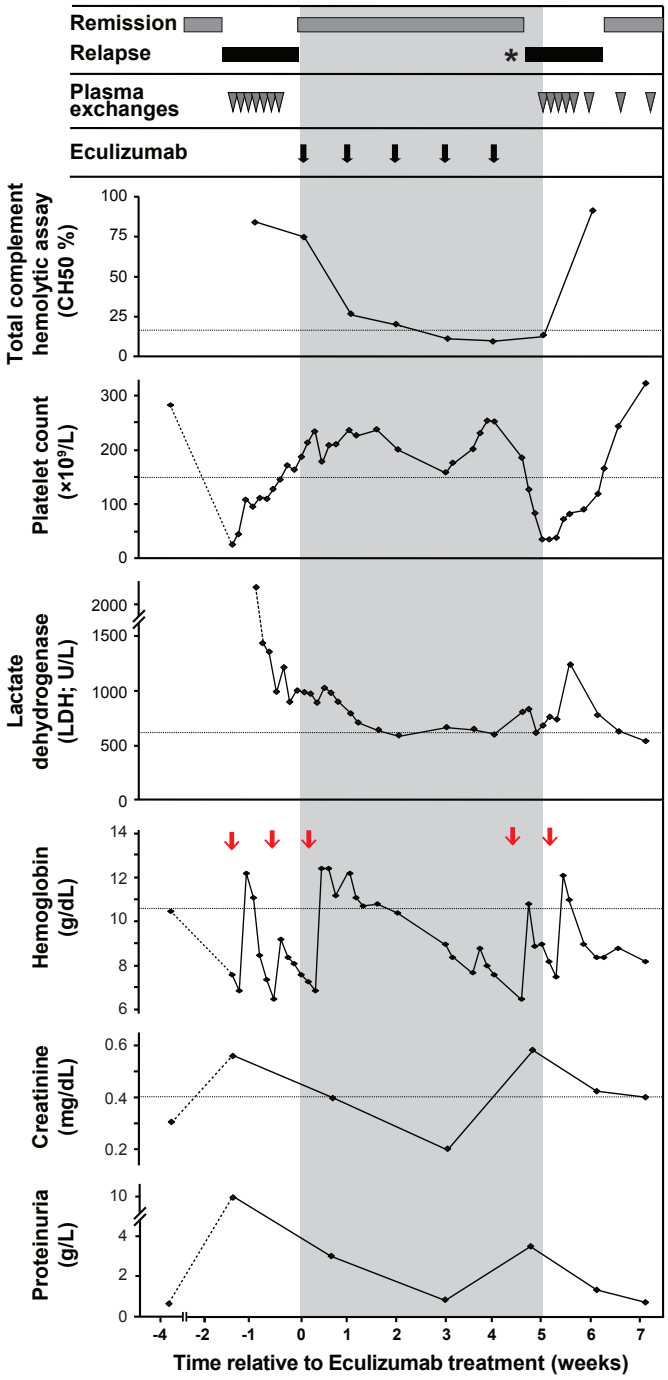

Supplementary Figure 5 HUS relapse while on eculizumab (anti-C5) therapy. Clinical values are shown for aHUS patient 6-3 over an 11-week period encompassing two HUS relapses, the second occurring during treatment eculizumab with therapeutic inhibition of complement cascade (CH50 < 15%). Values for CH50, platelet count, LDH, hemoglobin, creatinine and proteinuria are shown. The x-axis shows time, in weeks, relative to initiation of eculizumab treatment. The shaded gray area represents the eculizumab treatment period, with the timing of eculizumab infusions shown by black arrows. Gray arrowheads show the timing of plasma exchange therapy. The red arrows within the hemoglobin panel illustrate the timing of blood transfusions. Horizontal dashed lines show the lower limit of normal for platelets and hemoglobin and the upper limit for LDH and creatinine specific for age (1-2 year) and gender (female). For CH50 the dashed line denotes the therapeutic goal of CH50 < 15% normal. Before the transfusion during week 4, the absolute reticulocyte count was low, 22,000/mm^3 (normal range for non-anemic patients is 25,000-85,000/mm^3, accounting for the gradual hemoglobin decrease noted between week 0 and 4. The asterisk shows the onset of an influenza infection (top), confirmed by PCR, just before the HUS recurrence during week 4. At that time there was a rapid reduction in platelet count, an increase in proteinuria, creatinine, LDH and an increased rate of reduction of hemoglobin level after transfusion. These findings are indicative of aHUS relapse. CH50, total hemolytic complement activity; LDH, lactate dehydrogenase; PCR, polymerase chain reaction.

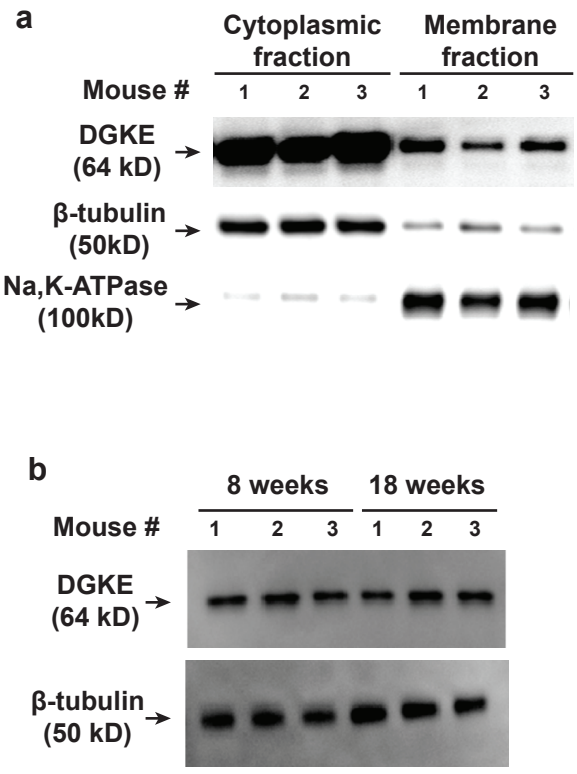

Supplementary Figure 6 Mouse platelets express high levels of DGKE protein that do not change with age. (**a**) Western blot shows that DGKE protein is present in both the cytoplasmic and membrane fractions of unstimulated platelets extracted from wild type C57/BL6 adult mice (50 micrograms of proteins were loaded in each lane). It also shows expression of β-tubulin and Na,K-ATPase, which are used both as loading controls and as controls for the efficiency of the subcellular fractionation: β-tubulin is enriched in the cytoplasm while Na,K-ATPase is enriched in the membrane fraction. (**b**) Western blot shows that DGKE protein is present in lysate of unstimulated platelets extracted from 8-week- and 18-week-old wild type C57/BL6 mice (50 micrograms of proteins were loaded in each lane). It also shows expression of β-tubulin, which is used as a loading control.

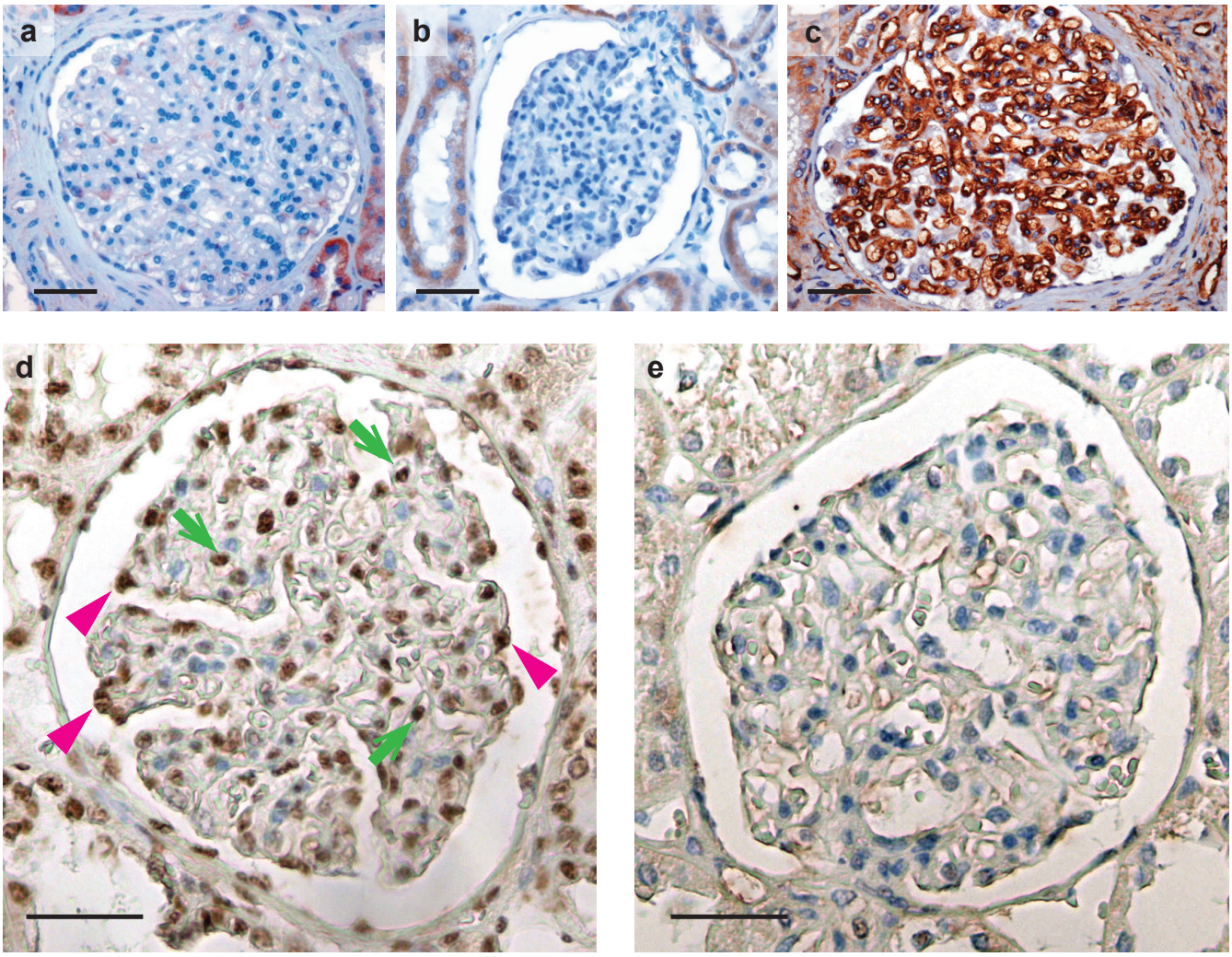

Supplementary Figure 7. Additional images for DGKE staining of normal and DGKE-mutant human kidneys. (**a**) Kidney specimen from aHUS patient 2-7, stained with polyclonal rabbit anti-DGKE antibody (Novus) and anti-rabbit-HRP, DAB reaction stopped after 30 min (DAB and hematoxylin). This long exposure shows slight staining in podocyte, consistent with incomplete degradation of the DGKE allele harboring a missense mutation in this patient. (**b**) Kidney of normal subject stained with rabbit isotype antibody as primary antibody followed by secondary antibody, DAB reaction stopped after 5 min (DAB and hematoxylin). Result shows no staining in absence of DGKE antibodies. (**c**) Kidney from aHUS patient 2-7, stained with monoclonal mouse anti-CD34 antibody (Dako) followed by secondary antibody, DAB reaction stopped after 5 min (DAB and hematoxylin). The pattern and intensity of the CD34 staining in the patient glomeruli is normal and robust, indicating that the absence of DGKE staining is not explained by poor tissue preservation. (**d**) Normal kidney (different subject than shown above and in **Fig. 4**) stained with monoclonal mouse anti-DGKE antibody (R&D) followed by secondary antibody, DAB reaction stopped after 15 min (DAB and hematoxylin). Examples of DGKE-positive endothelial cells and podocytes are indicated by green arrows and pink arrowheads, respectively. (**e**) Normal kidney stained with secondary antibody alone, DAB reaction stopped after 15 min (DAB and hematoxylin). No staining is seen. Scale bars, 50 μm for **a-e**.

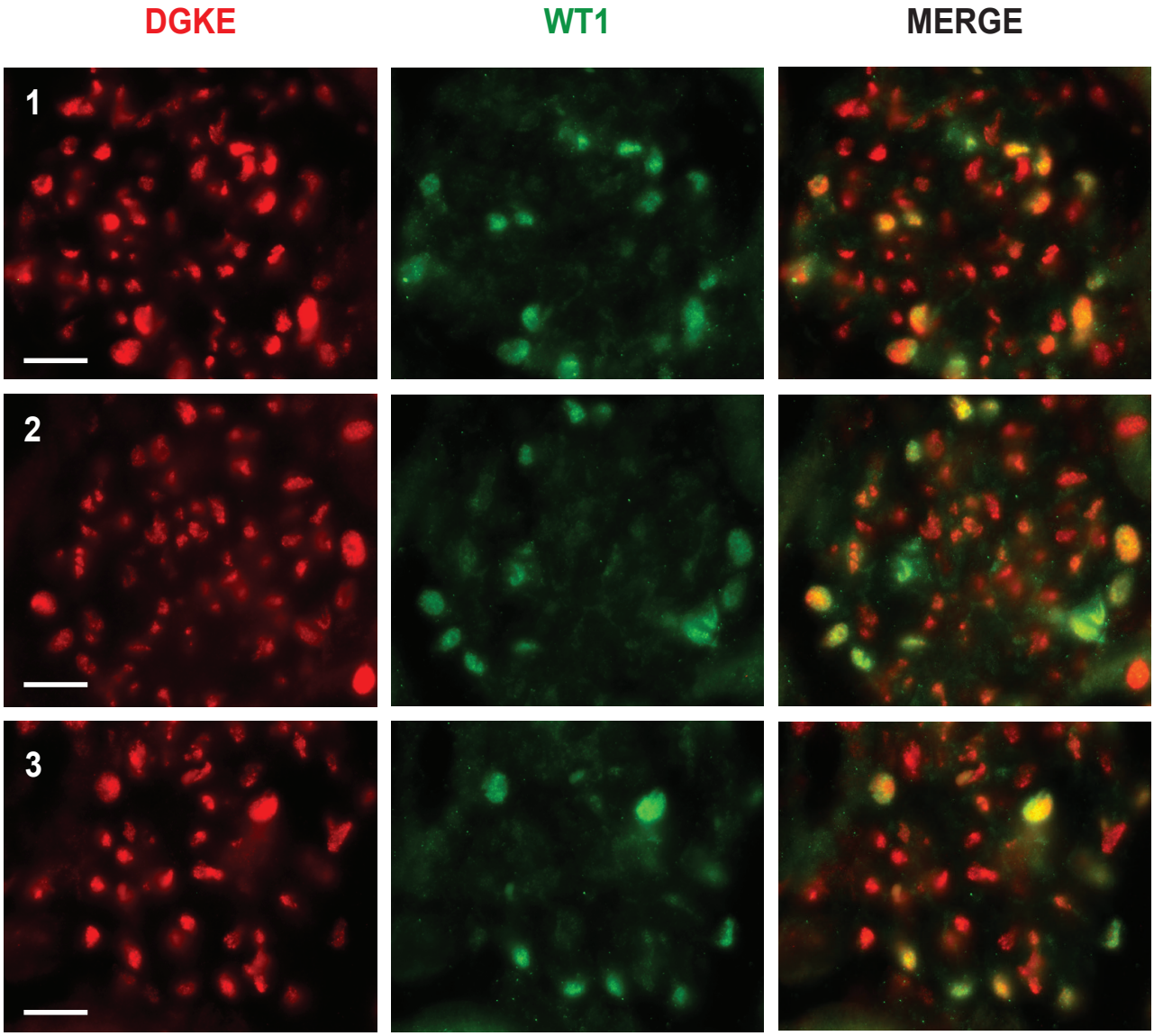

Supplementary Figure 8 Co-localization of DGKE and WT1 in rat glomeruli. Three representative examples of rat glomeruli stained with monoclonal mouse anti-DGKE (from R&D, shown in red) and polyclonal rabbit anti-WT1 (in green; from Santa Cruz) antibodies are shown. Cells that stain for WT1, a podocyte marker, also stain for DGKE. A substantial number that stain for DGKE but not WT1 are observed; per morphologic findings with immunohistochemistry in **Fig. 4** and **Supplementary Fig. 7**, many of these are endothelial cells. Staining with fluorescent-labeled secondary antibodies was consistently negative (data not shown). Scale bars, 20 μm for panels **1-3**.

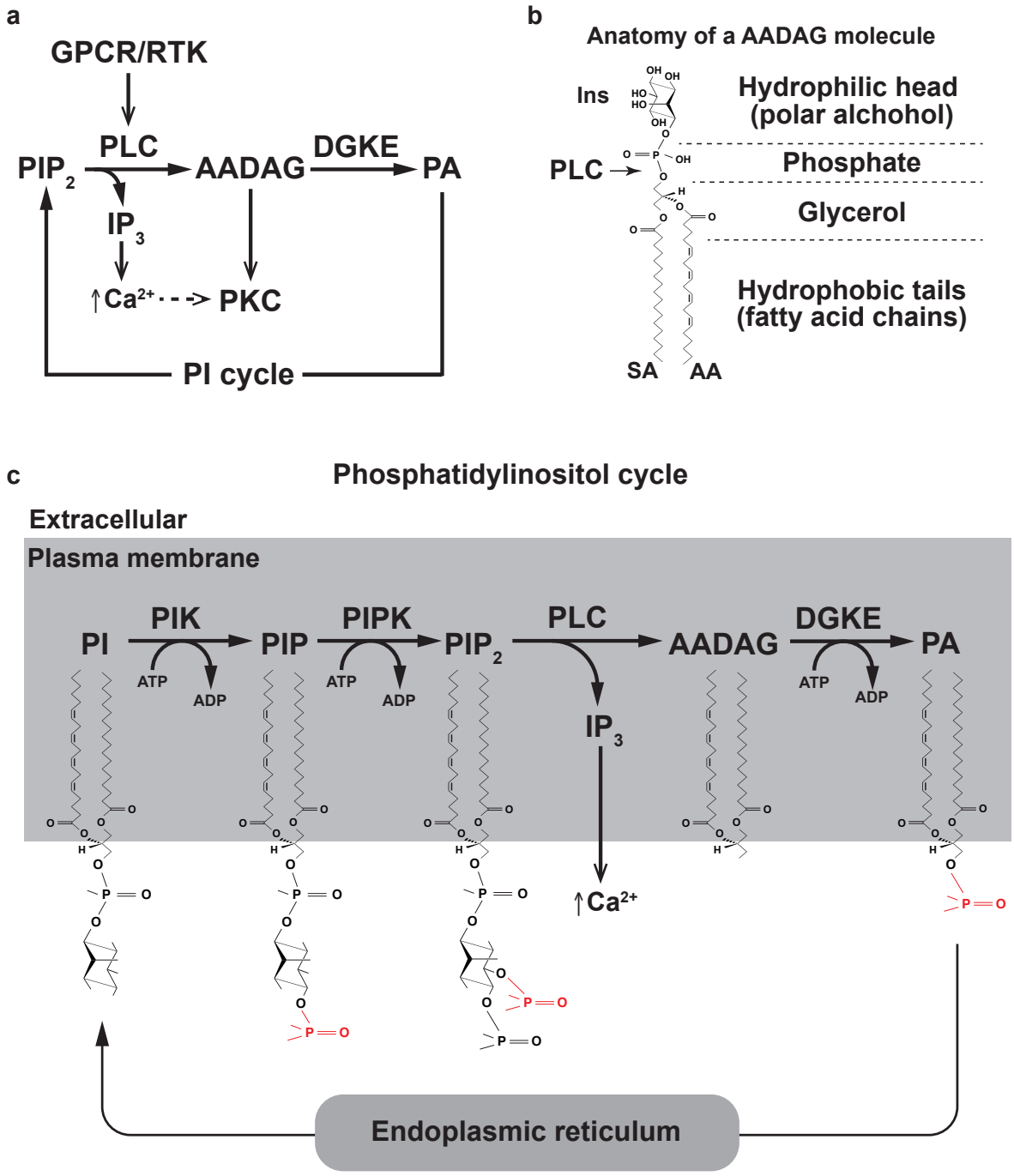

Supplementary Figure 9 DGKE regulates levels of AADAG in the phosphatidylinositol cycle. (**a**) Extracellular signals activate phospholipase C (PLC), which produces arachidonic acid-containing diacylglycerol (AADAG) from phosphatidylinositol 4,5-bisphosphate (PIP_2). AADAG signaling promotes protein kinase C (PKC) activity. AADAG signaling is terminated by their phosphorylation by DGKE to the corresponding phosphatidic acid (PA). PA is an obligatory intermediate in recycling AADAGs to PIP_2 via the phosphatidylinositol (PI) cycle (see panel **c**, below). (**b**) Structure of the most common AADAG containing arachidonic acid (AA) and stearic acid (SA) is shown. The site of PLC cleavage is indicated. (**c**) PI cycle regenerates PI from PA. PLC is regulated by activity of various G-protein coupled receptor (GPCR), receptor tyrosine kinase (RTK) and mechanical stimuli. AADAG is phosphorylated to PA by DGKs such as DGKE. The remainder of the cycle that ultimately regenerates PI takes place in the endoplasmic reticulum. ADP and ATP, adenosine di- and tri-phosphate; Ins, myo-inositol; IP_3, inositol 1,4,5-triphosphate; PIP, phosphatidylinositol 4-phosphate.

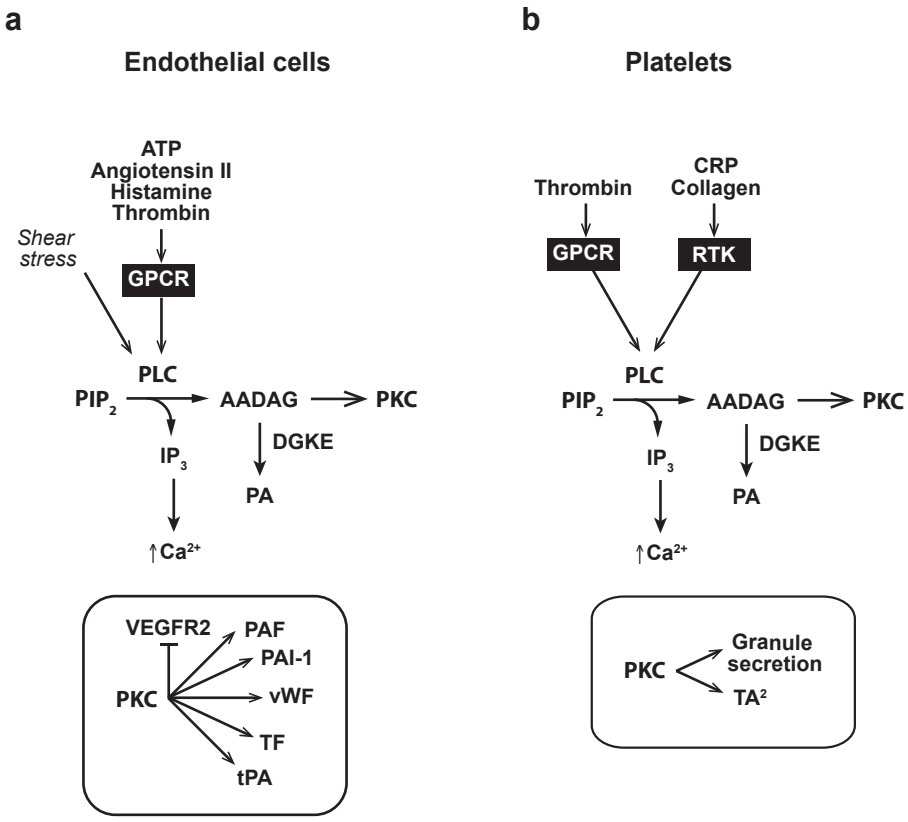

Supplementary Figure 10 DGKE potential roles in modulating PKC activity in endothelial cells and platelets. (**a-b**) Various physiological stimuli (italics) and ligands that activate PKC via their cognate GPCRs or RTKs are presented, and the consequences of PKC activation in endothelium (**a**) and platelets (**b**) are shown. (**a**) PLC activity is dramatically increased in response to membrane signaling via GPCR (receptors for ATP[1], angiotensin II[2], histamine[3], and thrombin[3]) and mechanical stimuli (sheer stress[4]). Inset shows that activation of PKC results in increased production of various pro- and anti-thrombotic factors (arrows) and decreased VEGFR2 trafficking to the plasma membrane (flat-headed arrow), as described in main text. (**b**) A similar increase in PLC activity is observed in response to membrane signaling via GPCR (receptors for thrombin[5]) and RTKs (CRP[6], collagen[7]). Inset shows that activation of PKC results in increase granule and TA_2 secretion. AADAG, arachidonic acid-containing diacylglycerol; ATP, adenosine triphosphate; CRP, collagen-related peptide; DGKE, diacylglycerol kinase epsilon; GCPRs, G-protein coupled receptor; PA, phosphatidic acid; PAF, platelet-activating factor; PAI-1, plasminogen activator inhibitor-1; PIP_2, phosphatidylinositol 4,5-bisphosphate; PKC, protein kinase C; PLC, phospholipase C; RTKs, receptor tyrosine kinase; TA_2, thromboxane A_2; TF, tissue factor; tPA, tissue plasminogen inhibitor, VEGFR2, vascular endothelial growth factor receptor-2; vWF, von Willebrand factor.

References for **Supplementary Figure 10**:

1. Wilkinson, G. F., et al. *Brit. J. Pharmacol.* **108**, 689-693 (1993).
2. Pueyo, M. E., et al. *Brit. J. Pharmacol.* **118**, 79-84 (2012).
3. Brock, T. A. & Capasso, E. A. *J. Cell. Physiol.* **136**, 54-62 (1988).
4. Bhagyalakshmi, A., et al. *J. Vasc. Res.* **29**, 443-449 (1992).
5. Offermans, S. *Circ. Res.* **15**, 1293-1304 (2006).
6. Asselin, J, et al. *Blood*. **89**, 1235-1242 (1997).
7. Keely, P. J. & Parise, L. V. *J. Biol. Chem.* **271**, 26668–26676 (1996).

Supplementary Table 1 Complement assessment and antibody profiling of pediatric patients with aHUS harboring homozygous or compound heterozygous variants in *DGKE*

Subject ID	Age when tested (yr)	CH50 (%) nl 70-130	C3 (mg/L) nl > 660	C4 (mg/L) nl > 93	CFB (mg/L) nl > 90	CFH (mg/L) nl > 338)	CFI (mg/L) nl > 42	MCP (MFI) nl > 600	sC5b-9 (ng/mL) nl < 420	Sheep erythrocytes lysis (%) nl < 10	Anti-CFH antibodies
1-3[a]	1	nd	1,690	nd	nd	643	60	1,020	nd	nd	neg
	9	102	857	193	139	637	66	nd	230	<10	nd
1-4	0.3	113	974	222	222	622	65	900	nd	<10	neg
2-5[a]	16	nd	700	nd	nd	500	60	1,024	nd	nd	neg
2-7[a]	10	nd	1,120	nd	nd	474	68	828	nd	nd	neg
	18	131	nd	321	224	nd	nd	nd	141	<10	nd
3-3[a]	1	nd	823	nd	nd	571	60	1,595	nd	nd	neg
	16	103	nd	416	123	nd	nd	nd	178	<10	nd
4-1[a]	15	nd	1,050	nd	nd	663	67	1,219	nd	nd	neg
	16	76	nd	220	90	nd	nd	nd	147	<10	nd
5-3[a]	1.3	nd	955	nd	nd	734	83	nd[b]	nd	nd	neg
6-3	0.5	nd	884	nd	nd	566	60	628	nd	nd	neg
7-3	0.9	70	625	301	142	439	97	1,040	244	<10	neg
	1	93	nd	132	136	nd	nd	nd	nd	nd	nd
8-3	3	84	705	132	122	826	103	1,027	241	<10	neg
9-3	15.5	nd	nd	nd	nd	469	42	nd	nd	nd	neg
9-4[a]	9	nd	880	nd	nd	831	68	nd	nd	nd	neg
9-6[a]	5.5	nd	1,090	nd	nd	668	54	nd	nd	nd	neg

C3, complement component 3; C4, complement component 4; CFB, Complement factor B; CFH, Complement factor H; CFI, Complement factor I; CH50, complement hemolysis 50; MCP, complement membrane cofactor protein; MFI, mean fluorescence intensity; sC5b-9, soluble complement factor 5b-9.

[a]The samples of these patients were not drawn during an acute episode of HUS and thus represent steady-state levels when asymptomatic; [b]MCP assessment were not routinely done when patient 5-3's sample was received; results are of this test are not reliable when done on frozen samples.

Supplementary Table 2 Additional clinical characteristics for the patients with *DGKE* nephropathy*

Kindred number		1		2		3	4	5	6	7	8		9	
Subject ID		1-3	1-4	2-5	2-7	3-3	4-1	5-3	6-3	7-3	8-3	9-3	9-4	9-6
Decade of birth[a]		2000's	2000's	1980's	1990's	1990's	1990's	2000's	2000's	2000's	2000's	1990's	2000's	2000's
Gender		M	F	F	F	F	F	M	F	M	M	M	M	F
Age at first HUS episode, months		8	4	7	4	6	4	7	6	11	8.5	4	9	3
Diarrhea at onset?		No	No	No	No	No	Yes	Yes	Yes	No[c]	Yes	No	No	No
LDH (nl < 150 IU/L)		2,065	3,280	nd	nd	nd	nd	16,000	3,142[d]	4,950	2,400	6,446	nd	2,500
Haptoglobin (nl < 0.4 g/L)		<0.1	<0.1	nd	nd[b]	nd	<0.1	nd	0.28	<0.1	<0.1	<0.1	nd	<0.1
Schistocytes on smear (nl = No)		Yes	Yes	Yes	Yes	Yes	Yes	nd	Yes	Yes	Yes	nd	nd	nd
Therapy at onset	Dialysis	Yes	Yes	No	No	No	Yes	Yes	Yes	Yes	Yes	Yes	No	Yes
	Plasmatherapy	No	Pex	FFP	No	No	FFP	No	Pex	Pex	Pex	FFP	No	FFP
	Immunotherapy	No	No	IVIG	No	No	No	No	No	No	No	No	No	No
Number of relapses		0	1	1	4	1	0	1	3	1	0	2	2	5
Therapy for relapses	Dialysis	NA	No	No	No	Yes	NA	No	No	No	NA	No	No	No
	Plasmatherapy	NA	Pex	No	Pex	Pex, FFP	NA	No	Pex	Pex	NA	No	FFP	FFP
	Immunotherapy	NA	Ec	No	No	IVIG CS	NA	CS MMF	Ec	Ec	NA	CS MMF	No	No
Diagnoses for additional renal biopsy (age at biopsy, yr)		TMA (9)	nd	TMA (3)	Fibrosis (21)	TMA (1, 5)	TMA (2, 4)	TMA (5)	TMA (3, 4)	nd	nd	nd	nd	nd
Renal outcomes	Hypertension	Yes	Yes	Yes	Yes	Yes	Yes	Yes	Yes	Yes	Yes	Yes	Yes	Yes
	Proteinuria	Yes	Yes	Yes, NS	Yes	Yes	Yes	Yes, NS	Yes	Yes	Yes	Yes, NS	Yes	Yes
	Hematuria	Yes	Yes	Yes	Yes	Yes	Yes	Yes	Yes	Yes	Yes	Yes	Yes	Yes
	Renal function	CKD1	CKD1	Tx	CKD4	CKD4	Tx	CKD1	CKD1	CKD1	Tx	HD	CKD1	CKD1
	HUS recurrence post-Tx	-	-	No	-	-	No	-	-	-	No	-	-	-
Maintenance therapy		Ec	Ec	No	Ec	No	No	No	Ec	Ec	No	No	FFP Ec	FFP Ec
# relapses while on maintenance		0	0	NA	0	NA	NA		1 (Ec)	0	NA	NA	0	1 (FFP)
Consanguinity		No	No	No	No	No	No	No	Yes	Yes	Yes	Yes	Yes	Yes

CKDx, chronic kidney disease, stage x; CS, corticosteroids; Ec, eculizumab (anti-C5 antibody); FFP, fresh frozen plasma; HD, hemodialysis; IVIG, intravenous immunoglobulin; LDH, lactate dehydrogenase; MMF, mycophenolate mofetil; MPGN, membranoproliferative glomerulonephritis; NA, not applicable; nd, not done; nl, normal; NS, nephrotic syndrome; Pex, plasma exchange therapy; TMA, thrombotic microangiopathy; Tx, renal transplantation.

*Reference values for infants <1 year of age, from Soldin (2005). [a]These data are given to provide context for the therapies used; therapeutic options have chnaged dramatically over the past 30 years. [b]haptoglobin < 0.1 g/L for all 4 subsequent relapses; [c]Initial clinical presentation was diagnosed during a H1N1 flu infection; [d]The normal range for LDH in the hospital where this patient has received care since diagnosis is < 670 U/L.

Supplementary Table 3 Summary of sequencing metrics for the exome capture of the affected siblings from kindreds 1 and 2

Parameters	Kindred 1		Kindred 2	
	1-3	1-4	2-5	2-7
Number of reads (million)	142.4	103.9	111.7	104.7
Median coverage (×)	135	98	104	98
Mean coverage (×)	157.1	115.9	122.8	115.6
Bases mapping to the genome (%)	90.2	89.7	90.8	90.8
Bases mapping to the exome (%)	73.3	74.5	72.5	72.9
Bases covered at least 4× (%)	97.7	97.5	97.7	97.6
Bases covered at least 8× (%)	96.9	96.5	96.8	96.6
Mean error rate (%)	0.67	0.71	0.51	0.52
% of PCR duplicate	5.59	4.41	5.70	5.31

Supplementary Table 4 Impact of filters applied to raw data to rare single nucleotide variants or insertion/deletions shared among sibling (data from chromosomes X and Y not included)*

Filters	Kindred 1				Kindred 2			
	Heterozygous		Homozygous		Heterozygous		Homozygous	
	1-3	1-4	1-3	1-4	2-5	2-7	2-5	2-7
Greater than quality score thresholds[a]	21,906	21,323	13,170	12,918	28,520	28,417	13,869	13,608
Not part of a segmental duplication > 1,000 bp	19,892	19,419	12,326	12,094	26,156	26,009	12,959	12,753
Protein altering variants (including indels)	5,010	5,004	3,151	3,072	6,460	6,465	3,283	3,227
MAF thresholds in Yale/NHLBI exomes or 1000 Genomes[b]	44	47	4	1	237	233	2	5
Damaging and conserved missense variants	33	38	4	1	181	185	2	4
Variants shared between affected siblings	16		1[c]		91		1[e]	
Number compound heterozygous variants	0		N/A		1[d]		N/A	
Variants in same gene between families	1							

MAF, minor allele frequency.

*dbSNP database was not used as a filter. [a]Quality score thresholds: heterozygous SNV calls QS>100, homozygous SNV calls QS>60. [b]Minor allele frequency cut-off is 0.1% for heterozygous variants and 1% for homozygous variants. [c]Homozygous *DGKE* pTRP.322*. [d]Compound heterozigosity for *DGKE* p.Arg63Pro and *DGKE* p.Val163Serfs*3. [e]*OR6Y1* (olfactory receptor, family 6, subfamily Y, member 1), p.Pro68* (rs149371181).

Supplementary Table 5 Mapping the boundaries of the homozygous segments and length of the shared haplotype segment for 3 subjects with homozygous *DGKE* p.Trp322* using genotyping of common variants

SNP # on Suppl. Fig. 2	SNP rs #*	Position on chr 17 (base)		Position on chr 17 (cM)[c]	Distance (kb) from W322*	HW p-value[a]	HapMap MAF[a]	Genotype data for[d]		
		Hg18[a]	Hg19[b]					1-3	4-3	8-3
-	rs6503934	43,368,649	46,013,650	68.602279[e]	-8,912.5	0.90	0.41	ND	ND	T/**C**
-	rs4793996	44,374,596	47,019,597	68.979469	-7,906.6	0.91	0.46	ND	ND	C/C
-	rs12451482	45,075,097	47,720,098	70.070992[e]	-7,206.0	1.00	0.50	ND	ND	**T/T**
-	rs2586465	45,780,966	48,425,967	71.764626	-6,500.2	1.00	0.42	ND	ND	T/T
-	rs7209022	46,993,753	49,638,754	73.369661	-5,287.4	0.45	0.39	ND	ND	A/A
-	rs1553368	49,004,170	51,649,171	74.742026	-3,277.0	0.98	0.45	ND	ND	**G/G**
-	rs12603570	50,954,716	53,599,717	76.841411	-1,326.4	0.50	0.48	ND	ND	**C/C**
-	rs8069322	51,805,133	54,450,134	78.065219[e]	-476.0	0.13	0.25	**A/A**	G/**A**	G/G
-	rs10852985	51,889,633	54,534,634	78.084464	-391.5	0.40	0.24	**A/A**	G/**A**	G/G
-	rs1545261	51,935,771	54,580,772	78.123342	-345.4	0.84	0.11	**C/C**	**C/C**	**C/C**
-	rs12450049	51,951,225	54,596,226	78.124427	-0.330	0.69	0.33	G/**A**	G/**A**	**A/A**
-	rs103395	52,051,231	54,696,232	78.463311	-230.0	1.0	0.18	**A/A**	**A/A**	**A/A**
-	rs7208197	52,056,582	54,701,583	78.465832	-224.6	1	0.085	**G/G**	**G/G**	**G/G**
-	rs4605230	52,059,828	54,704,829	78.469067	-221.3	0.47	0.37	**T/T**	A/A	**T/T**
-	rs12325830	52,064,643	54,709,644	78.470051	-216.5	0.04	0.45	T/T	**C/C**	T/T
-	rs227665	52,168,750	54,813,751	78.734307	-112.3	0.13	0.30	**A/A**	**A/A**	**A/A**
-	rs227662	52,170,563	54,815,564	78.745934	-110.6	1	0.18	**C/C**	**C/C**	**C/C**
-	rs8069500	52,173,224	54,818,225	78.7538	-107.9	1	0.39	C/C	C/C	C/C
-	rs3914804	52,175,260	54,820,261	78.761973	-105.9	0.71	0.30	A/A	A/A	A/A
140	rs17822403	52,224,472	54,869,473	79.037843	-56.7	1	0.17	T/T	T/T	T/T
144	rs3853823	52,231,863	54,876,864	79.039351	-49.3	0.06	0.19	A/A	A/A	A/A
156	rs2235092	52,266,928	54,911,929	79.043373[e]	-14.2	0.35	0.35	G/G	G/G	G/G
157	rs7225724	52,267,736	54,912,737	79.044395	-13.4	1.00	0.11	**G/G**	**G/G**	**G/G**
158	rs6503772	52,271,688	54,916,689	79.045028	-9.4	1.00	0.45	A/A	A/A	A/A
-	p.Trp322X	52,281,133	54,926,134	-	-	-	-	-	-	-
162	rs4794670	52,282,828	54,927,829	79.045647	+1.7	0.16	0.26	**A/A**	**A/A**	**A/A**
164	rs11651692	52,293,014	54,938,015	79.046361	+11.9	0.34	0.30	**G/G**	**G/G**	**G/G**
168	rs7209070	52,301,193	54,946,194	79.047342	+20.1	0.58	0.29	**C/C**	**C/C**	**C/C**
-	rs2525997	52,326,240	54,971,241	79.25804	+45.1	1	0.107	C/C	C/C	C/C
-	rs205499	52,327,400	54,972,401	79.271336	+46.3	0.62	0.158	**G/G**	**G/G**	**G/G**
-	rs205498	52,333,793	54,978,794	79.322774	+52.7	0.34	0.25	**A/A**	**A/A**	**A/A**
215	rs2301823	52,393,489	55,038,490	79.361959[e]	+112.4	0.9117	0.474	**A/A**	**A/A**	**A/A**
219	rs7221286	52,409,153	55,054,154	79.363312[e]	+128.0	0.5471	0.282	**C/C**	**C/C**	**C/C**
225	rs12453004	52,420,529	55,065,530	79.365252	+139.4	0.40	0.60	**G/G**	**G/G**	**G/G**
229	rs17833633	52,431,759	55,076,760	79.370538	+150.6	0.29	0.48	C/C	C/C	C/C
-	rs917927	52,505,204	55,150,205	79.818432	+224.1	1.0	0.45	G/G	**T/T**	**T/T**
-	rs1007462	52,558,314	55,203,315	79.903638	+277.2	0.39	0.46	T/T	**C/C**	**C/C**
-	rs4794707	52,595,599	55,240,600	79.944243	+314.4	0.67	0.34	**A/A**	C/C	C/C
-	rs3744089	53,057,256	55,702,257	81.424977	+776.0	1	0.21	**T/T**	C/C	**T/T**
-	rs6503825	53,072,744	55,717,745	81.452585	+791.6	0.90	0.50	C/**T**	**T/T**	C/**T**
-	rs10083864	53,192,909	55,837,910	81.658245	+911.8	1	0.46	C/**T**	C/C	C/C
-	rs2233906	53,440,438	56,085,439	82.403671	+1159.3	0.40	0.15	**T/T**	C/C	**T/T**
-	rs3863502	53,588,498	56,233,499	82.566118	+1307.4	0.86	0.44	**C/C**	**C/C**	**C**/T
-	rs60994383	53,602,100	56,247,101	82.647271[e]	+1320.9	N/A	N/A	**C**/A	**C**/A	**C/C**

*All variants were identified using Haploview 4.2 (version 3; release R2; analysis panel CEU). [a]These data were extracted directly from the Haploview output files ("HapMap download" option). [a]The SNP coordinates from Haploview 4.2 were converted from Hg18 to Hg19 using UCSC Genome Browser LiftOver function. [c]The positions in centimorgans (cM) were obtained from HapMap Phase II genetic map (Hg19). [d]We report genotyping data at each locus relative to the positive strand, and major alleles (frequency > 50%) are in bold font. [e]Since these SNPs are not part of HapMap Phase II, the closest HapMap Phase II SNP position is indicated. The boundaries of the shared segment is indicated by the lines. The extent of each patients' homozygous segment is indicated in shaded gray.